

## Analysis and Simulation of Narrow Band Digitally Beamformed Phased Array Antenna with Null Steering

Ahmed Najah Jabbar, M.Sc. in electronic and communication ENG.

### ABSTRACT:

This paper illustrates the analysis and simulation of narrow band antenna arrays with adapted radiation pattern using digital beamformation. The technique used for the system is the Shifted Sideband Beamformer (SSB). This paper analyzes the stages of the receiver and presents a model for simulation. The SSB was chosen because it exhibits moderate complexity and storage requirement. Different spatial filters such as Uniform weight, Blackman-Harris, Tylor, and Dolph-Chebyshev were used to control the side lobe level of the arrays. This paper also shows how to implement null steering procedure to circumvent the jamming and high interference angles. Only the linear and two dimensional arrays were taken into consideration.

**Keywords:** Digital Beamforming, Digital Signal Processing, Smart Antennas, Phased Array Antenna, Wireless Communication, Linear and 2-D Antenna Array Receiver.

هذا البحث يبين تحليل ومحاكاة مصفوفة هوائيات ضيقة النطاق ذات نمط حزمة مكيف رقمياً. التقنية المستخدمة في المنظومة والتي تم تحليلها هي الحزمة الطرفية المزحفة. البحث يحلل مراحل منظومة الاستقبال ويفترض نموذجاً لغرض المحاكاة. اختيرت تقنية الحزمة الطرفية المزحفة لأن هذه التقنية ذات تعقيد ومتطلبات خزن معتدلة. أُستُخدمت مرشحات مكانية مختلفة مثل بلاكمان-هاريس، تايلور، ودولف-تشيبشيف للسيطرة على مستوى الفصوص الجانبية للمصفوفة. البحث أيضاً يبين كيفية استخدام أسلوب توجيه النقاط الصفيرية باتجاه التشويش والإشارات المتداخلة عالية القيمة لتقليل أثرها. المصفوفات من نوع أحادية البعد وثنائية البعد فقط أخذت بنظر الاعتبار.

### 1. Introduction:

Digital beamforming (DBF) is a method to steer the main lobe of Phased Array Antenna (PAA) in a certain desired direction. The early concept underlying digital beamforming was developed for applications in sonar and radar systems. DBF represent a quantum step in antenna performance and complexity [Litva and Lo 1996, Krieger, *et. al.* 2008]. In a DBF antenna system, the received signals are detected and digitized at the element level. By capturing the RF information in the form of digital stream, the door is opened for a large domain of signal processing techniques used to extract the information from the spatial domain data [Litva and Lo 1996, Allen and Ghavami 2005]. DBF is considered as an optimum antenna because all data at the face of the antenna are processed without introducing any distortion.

Eventually one would expect that the receiver would be built using software rather than hardware. The main advantage of DBF is its flexibility to manipulate data without degrading the SNR.

In many cases it is considered as the ultimate antenna because all the information arrived at its face are captured without loss. The adopted algorithm in this paper is SSB due its low storage requirements and moderate complexity [Godara 1997, Mucci 1984, Li and Ghuang 2004]. Three main issues are important to the beamformation which are: 1-Mainlobe rotation, 2-Sidelobe level control, and 3- Null steering. The 1 and 2 issues are tightly connected as will be seen later.

## 2. The Mathematical DBF Receiver Model:

The DBF receiver consists of two parts: the Analog part (LNA and frequency transfer stage), and the digital part (ADC, Digital Down Converter (DDC), and the DSP).

### 2.1 Frequency-Wavenumber of the Array:

Consider the DBF receiver of  $N$ - elements shown in Fig. (1). Each element is separated from the other by  $d$ . The position vector  $\vec{p}_n$  for each element is given by [Rosario 2005, Van Trees]

$$\vec{k} = \frac{2\pi}{\lambda} \begin{bmatrix} \sin \theta \cos \varphi \\ \sin \theta \sin \varphi \\ \cos \theta \end{bmatrix}, \quad \vec{p} = \begin{bmatrix} p_x \\ p_y \\ p_z \end{bmatrix} \quad (1)$$

where  $\theta$  and  $\varphi$  are the azimuth and elevation incidence angles respectively.

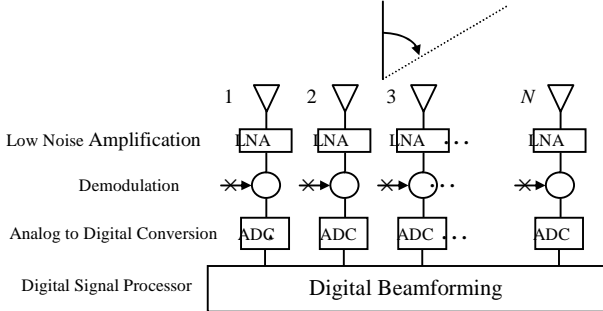


Fig. (1) Digital beamformer receiver block diagram

The incident plane wave on the sensors can be represented as:

$$f(t, \vec{p}_n) = x(t - \tau_n) \cos(\omega_{RF}(t - \tau_n)), \quad n=0, 1, \dots, N-1 \\ \approx x(t) \cos(\omega_{RF}t - \theta_n) \quad (2)$$

Where:  $\tau_n$ : is the time delay for the  $n^{th}$  element

$x(t)$ : the received signal

$\omega_{RF}$ : is the  $RF$  frequency of the received signal

$$\theta_n = \omega_{RF} \tau_n \quad (3)$$

The LNA is required because the signal arrived, normally, has a very low power. The LNA amplifies this signal to a level suitable for further processing by the next stages.  $RF$  is the modulation frequency. In many cases it is much higher than the sampling frequency of the ADC. Hence, we need to down convert  $RF$  to a value adequate for the ADC. The second stage (demodulation stage) carries out this

conversion. This stage has a Local Oscillator with frequency  $\omega_{LO}$ , thus, the output signal is [Rosario 2005, Shenghua *et. al.* 2005]

$$g'(t) = x(t)\cos(\omega_{RF}t - \theta_n)\cos(\omega_{LO}t) \quad (4)$$

Using trigonometric properties Eq. (4) becomes

$$g'(t) = \frac{x(t)}{2} [\cos(\omega_{IF}t - \theta_n) + \cos(\omega_{IM}t - \theta_n)] \quad (5)$$

where:  $\omega_{IF} \stackrel{\Delta}{=} \omega_{RF} - \omega_{LO}$ ,  $\omega_{IM} \stackrel{\Delta}{=} \omega_{RF} + \omega_{LO}$

If a passband filter with gain  $G=2$  is used to extract  $\omega_{IF}$ , the output signal obtained is:

$$g_n(t) = x(t)\cos(\omega_{IF}t - \theta_n) \quad (6)$$

The angular displacement, which represents the time delay of the incoming plane wave between the antennas of the array, is left unchanged in a modulation operation.

## 2.2 The ADC, DDC, and DSP Stage:

After the incoming signal in an antenna channel has been demodulated into an intermediate frequency and the signal of higher frequency is at least half as small as the sampling frequency, the ADCs with a sampling rate  $T_S$  can be used to transform the signal into a digital representation, as given in Eq. (7):

$$g_n[m] = x[m]\cos[\omega_{IF}m - \theta_n] \quad (7)$$

where  $t=mT_S$

After the antenna, the signal has been successfully sampled into the digital domain. The signal needs to be processed by the *first stage of the DBF receiver*, which is the Digital Down-Converter (DDC). The DDC is performed by multiplying the digital signal with a sinusoidal signal and a 90° phase-shifted version of the sinusoidal signal, both generated by digital local oscillator. The mathematical operations can be shown as:

$$i'_n[m] = x[m]\cos[\omega_{IF}m - \theta_n]\cos[\omega_{DLO}m] \quad (8)$$

$$q'_n[m] = x[m]\cos[\omega_{IF}m - \theta_n]\sin[\omega_{DLO}m] \quad (9)$$

If the Digital Local Oscillator frequency  $\omega_{DLO} = \omega_{IF}$ , then:

$$i'_n[m] = \frac{x[m]}{2} (\cos[2\omega_{IF}m] + \cos[\theta_n]) \quad (10)$$

$$q'_n[m] = \frac{x[m]}{2} (\sin[2\omega_{IF}m] + \sin[\theta_n]) \quad (11)$$

The final step in DDC is using filter with  $G=2$  to extract the phase component. The output of the filter is:

$$i''_n[m] = x[m]\cos[\theta_n] \quad (12)$$

$$q''_n[m] = x[m]\sin[\theta_n] \quad (13)$$

The block diagram of the *RF demodulator* and the DDC stage for each antenna channel in the PAA is shown in Fig. (2),

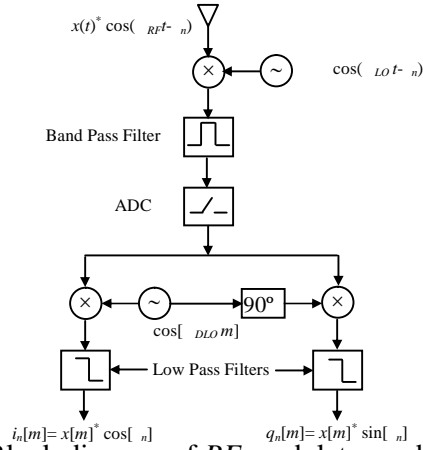


Fig. (2) Block diagram of RF modulator and DDC

The second stage of the DBF receiver is the Complex Weight Multiplication (CWM) stage. In this stage, the complex weight  $w_n^*$  associated with each antenna channel in the PAA is multiplied by the digital baseband signals  $i_n[m]$  and  $q_n[m]$ . To represent this complex multiplication operation, a signal  $b_n[m]$  will be defined which is composed of the signals  $i_n[m]$  and  $q_n[m]$ :

$$b_n[m] = i_n[m] - jq_n[m] = x[m]e^{-j\theta_n} \quad (14)$$

It can be seen that the defined signal  $b_n[m]$  is basically the signal  $x[m]$  multiplied by a complex constant with an associated phase  $\theta_n$ . To recover  $x[m]$ , the complex signal  $b_n[m]$  has to be multiplied by the complex conjugate of the complex constant. In other words, if the complex weight  $w_n^* = e^{j\theta_n}$ , then the product of the complex signal  $b_n[m]$  and the complex weight is equal to the signal  $x[m]$ :

$$y_n[m] = w_n^* b_n[m] = e^{j\theta_n} x[m] e^{-j\theta_n} = x[m] \quad (15)$$

The CWM stage of the DBF is shown in Fig. (3). The process is applied by means of multiplication and addition of real-value variables. To make such operations possible,  $w_n^*$  is represented in rectangular form

$$w_n^* = \text{Re}\{w_n^*\} + j\text{Im}\{w_n^*\} \quad (16)$$

Once  $w_n^*$  has been represented in rectangular form, the resulting signal  $y_n[m]$  is obtained by applying the following mathematical operations:

$$y_n[m] = w_n^* b_n[m] = r_n[m] + js_n[m] \quad (17)$$

where

$$r_n[m] = i_n[m]\text{Re}\{w_n^*\} + (-q_n[m])(-\text{Im}\{w_n^*\}) \quad (18)$$

$$s_n[m] = i_n[m]\text{Im}\{w_n^*\} + (-q_n[m])(\text{Re}\{w_n^*\}) \quad (19)$$

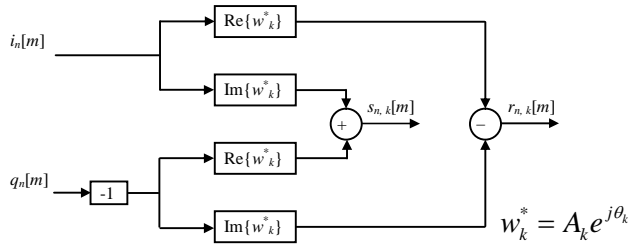


Fig. (3) Block diagram of CWM phase

The last stage is the summation of all  $y_n[m]$  values to produce  $y[m]$

$$y[m] = \frac{1}{N} \sum_{n=0}^{N-1} y_n[m] = \frac{1}{N} \sum_{n=0}^{N-1} r_n[m] + j \frac{1}{N} \sum_{n=0}^{N-1} s_n[m] = r[m] + js[m] \quad (20)$$

The term  $\frac{1}{N}$  is introduced to recover  $x[m]$  without gain.

The DSP can be constructed using different technologies. We can use either FPGA or dedicated processor for this operation. The use of FPGA provides parallel processing for each channel branch. A single processor can also be used as Multiply ACcumulate MAC to perform this operation. The techniques selected for this operation depends on the cost and the speed of operation for the system. Also multiple processors can be used.

### 2.3 The CIC filter

In a multirate DBF receiver; Cascaded Integrator-Comb (CIC) filter can be implemented to provide the synchronization. The CIC is a linear phase FIR filter implemented without the use of multiplication operations operating as a multirate filter to connect two signal processing system components operating at different sampling frequencies. Its name is derived from its structure, which consists of an integrator section operating at a high sampling rate combined with a comb section operating at a low sampling rate. CIC filters can be used to implement decimation and interpolation filters. Fig. 4 shows the architecture of a CIC decimation filter. The CIC filter design parameters are the rate change factor of the multirate filter ( $R$ ), the number of tap delays in each comb stage ( $M$ ), and the number of stages in the integrator and comb section of the filter ( $N$ ). The transfer function of the CIC filter referenced to the high sampling rate is a result of the multiplication of the transfer function of the integrator section and transfer function of the comb section [Rosario 2005, Schuler *et. al.* 2005, Swanson 2000]:

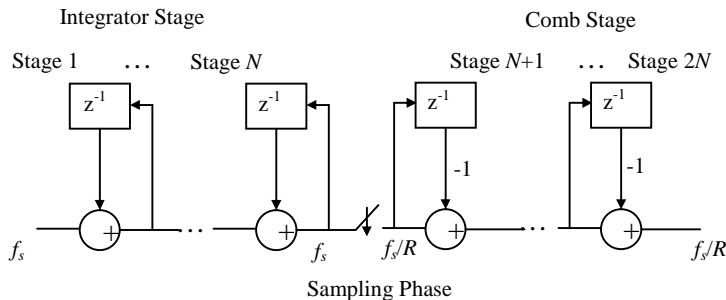


Fig. (4) Architecture of CIC filter

The power frequency response of the CIC filter relative to the low sampling rate is given by:

$$P(f) = \left[ \frac{\sin(\pi M f)}{\sin\left(\frac{\pi f}{R}\right)} \right]^{2N} \quad (21)$$

The magnitude and phase response is shown in Fig. (5) for  $R=10$ ,  $M=1$ , and  $N=10$  Versus normalized frequency

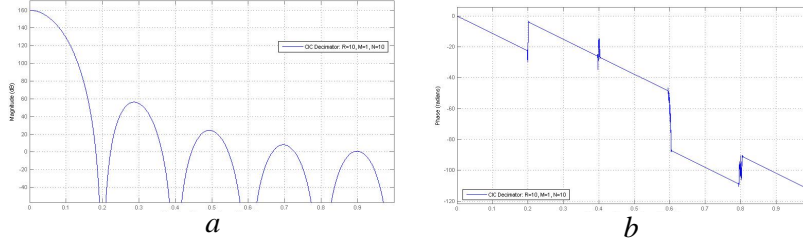


Fig. (5): (a) Magnitude response, (b) Phase response

The arrangement of the CIC filter with the DBF receiver is shown in Fig. (6)

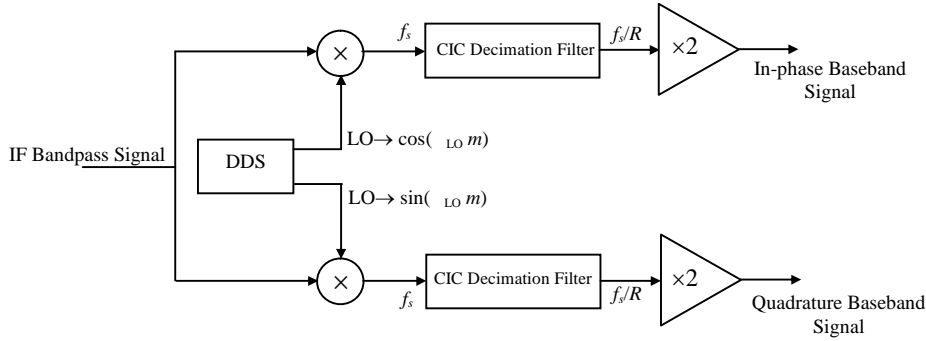


Fig. (6) Arrangement of CIC with DBF receiver

## 2.4 Narrow Band Beamformer

In this section we shall discuss the narrow band beamformation. A general characterization of the signal  $f(t, \mathbf{p})$ , where a bandpass signal is used to transmit information, can be described in the following form:

$$f(t, \mathbf{p}_n) = \sqrt{2} \operatorname{Re} \left\{ \tilde{f}(t, \mathbf{p}_n) e^{j\omega_c t} \right\}, \quad n=0, \dots, N-1 \quad (22)$$

If the signal  $f(t, \mathbf{p})$  is a plane-wave, the Eq. (22) can be simplified to:

$$f(t, \mathbf{p}_n) = \sqrt{2} \operatorname{Re} \left\{ \tilde{f}(t, \mathbf{p}_n) e^{j\omega_c (t - \tau_n)} \right\}, \quad n=0, \dots, N-1 \quad (23)$$

where

$$\tau_n = \frac{\bar{\mathbf{k}}^T \cdot \bar{\mathbf{p}}_n}{\omega_c} \quad (24)$$

An important parameter in the design of an array is  $\Delta T_{max}$ , which is the maximum travel time of a plane wave between any two elements of the array. If the mathematical description of the position of the elements of the array satisfies

$$\sum_{n=0}^{N-1} p_n = 0 \tag{25}$$

Which represents the elements of gravity to avoid grating [Van Trees 2002], then,

$$\tau_n \leq \Delta T_{max}, \quad n=0, \dots, N \tag{26}$$

The signal is defined as a narrowband signal if and only if

$$\Delta T_{max} \cdot B_s \ll 1 \tag{27}$$

where:  $B_s$  is the signal bandwidth

### 3. Linear Array DBF Receiver

There are two types of linear arrays: 1. Uniform Linear Array (ULA), and 2. Nonuniform Linear Array (NLA). We will concentrate the work on the ULA as it is most popular arrangement [Allen and Ghavami 2005, Rosario 2005, Wirth 2001]. The ULA are also classified into two Types: 1. Odd Elements Number, and 2. Even Elements Number. Fig. (7) shows examples of linear array arrangements along the z-axis. The  $\overline{p_n}$  for these arrays is [Rosario 2005, Van Trees 2002]

$$p_{zn} = \left( n - \frac{N-1}{2} \right) d \tag{28}$$

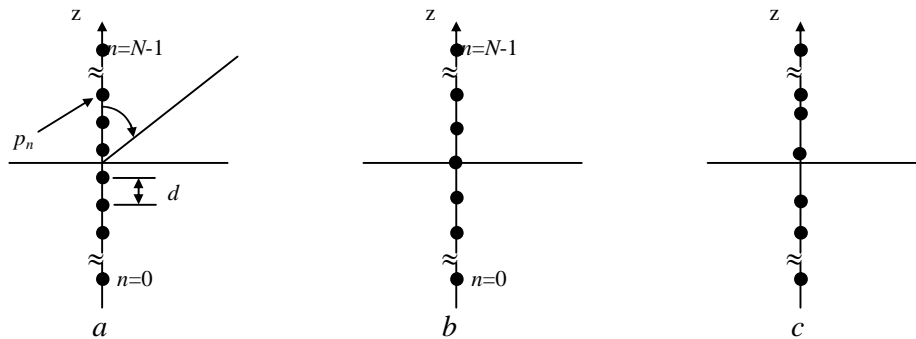


Fig. (7) Linear array arrangements (a) ULA with even elements number (b) ULA with odd elements number (c) NLA.

An example of 4- elements and 16-elements ULA will be given

#### 3.1 Simulation of (4 and 16)-Elements Array with Uniform Weighting:

The linear PAA Receiver Prototype consists of 4, 16 isotropic radiating antennas arranged in a linear distribution and uniformly spaced by half-wavelength. The operating carrier frequency of the PAA is 5.85 GHz. The intermediate carrier frequency (where the ADCs sample the incoming signal) of the DBF is 3 MHz. The incoming signal's bandwidth specification is 2 MHz. Since the Narrowband Factor ( $B_s \cdot \Delta T_{max} \approx 5.1282 \times 10^{-4}$ ) is extremely small compared to 1, a narrowband beamformer can be used to control the beam pattern of the array. The DDC operates at the sampling frequency of the ADC, which is 200 MHz. Each DDC contains two CIC filters (one for each quadrature channel) with 8 stages ( $N = 8$ ), a differential delay of 2 samples ( $M = 2$ ), a rate change factor of 4 ( $R = 4$ ) and a latency of 8 clock cycles. The CWM operates

at a sampling frequency of 50 MHz, which is the sampling frequency at the output of the CIC decimation filter. The resolution of the weight coefficient's amplitude is 16 bits with 14 bits of decimal precision and the weight coefficient's phase is 8 bits with no decimal precision. The output of the sine/cosine table in the CWM gives a bit resolution of 8 bits with 7 bits of decimal precision. The Main Response Axis (MRA) is  $MRA = 100^\circ$ . A uniform amplitude weight function is used. The polar and rectangular response of 4- and 16 elements are shown in Figs.(8, and 9) respectively

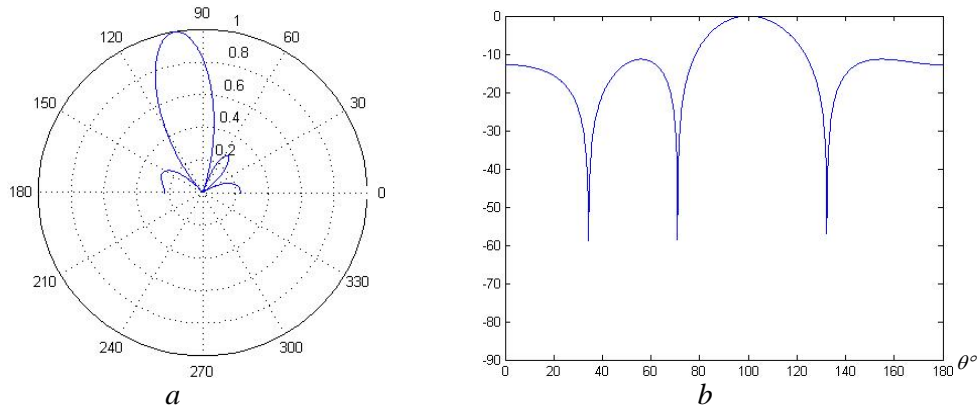


Fig. (8) Radiation pattern of 4-elements PAA with uniform Amplitude weighting  $MRA = 100^\circ$ , (a) Polar plot, (b) Rectangular plot

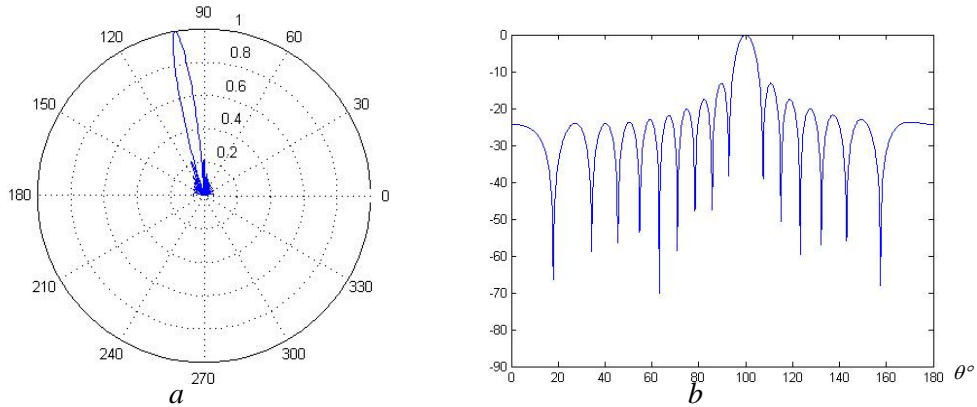


Fig. (9) The beam pattern of 16-elements PAA with uniform Amplitude weighting  $MRA = 100^\circ$ , (a) Polar plot, (b) Rectangular plot.

The complex weights of the 4-elements and 16-elements PAA are shown in Tables 1, and 2 respectively. Note that the argument of the weights is 0.25, 0.0625 respectively which equals to  $1/N$ .

Table 1 Complex weights of 4-element PAA ( $i = \sqrt{-1}$ )

Element	Value	Element	Value
1	$0.171 + i 0.183$	3	$0.241 - i 0.067$
2	$0.241 + i 0.067$	4	$0.171 - i 0.183$

Table 2 Complex weights of 16-element PAA

Element	Value	Element	Value	Element	Value	Element	Value
1	-0.036 -i 0.051	5	-0.021 +i 0.059	9	0.06 - i 0.017	13	-0.048 - i 0.04
2	-0.058 - i 0.025	6	0.013 + i 0.061	10	0.043 - i 0.046	14	-0.062-i 0.009
3	-0.062 +i 0.009	7	0.043 + i 0.046	11	0.013 - i 0.061	15	-0.058+i 0.025
4	-0.048 + i 0.04	8	0.06 + i 0.017	12	-0.021 - i 0.059	16	-0.036+i 0.051

One important measure of the array performance is the *directivity* [Van Trees 2002, Li and Stoica 2006]. For uniform weight ULA, it can be proven that the directivity  $D$  is:

$$D = N \tag{29}$$

Hence the directivity for the arrays is, 6.0205 and 12.0395 respectively.

### 3.2 Simulation of (4 and 16)-Elements Array with Taylor Amplitude Weighting Function:

Taylor developed a technique that constrains the maximum sidelobe height and gives decaying outer sidelobe. It can be applied to linear arrays by sampling the aperture weighting or by root-matching. Taylor started with uniform aperture weighting then moving the inner zeros to a new location on the unit circle in order to lower the *inner* sidelobes and leaving the *outer* zeros in same location. Taylor method aims to minimize the beamwidth based on sidelobe level specification. The position of the nulls in  $\theta$ -space for Taylor weight distribution can be described in the following mathematical form [Van Trees 2002, Li and Stoica 2006]:

$$\psi_n = \frac{2\pi}{N} \left\{ n \left[ \frac{A^2 + \left(n - \frac{1}{2}\right)^2}{A^2 + \left(\frac{-n}{2}\right)^2} \right]^{\frac{1}{2}} \right\} \tag{30}$$

where  $n$  is the number of inner zeros in the beam pattern and  $A$  is related to the maximum sidelobe height  $R$  by the following equation:

$$\cosh(\pi A) = R \tag{31}$$

The simulation results for the 4 and 16-elements PAA are shown in Figs. (10, 11) respectively

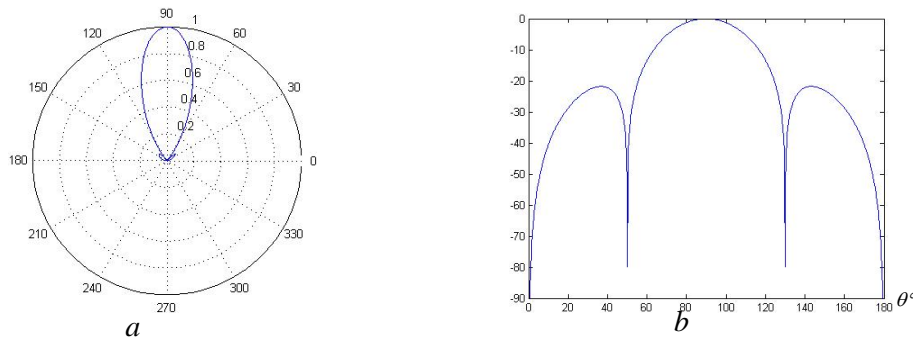


Fig. (10) The beam pattern of 4-elements PAA with Taylor Amplitude weighting  $MRA=90^\circ$ , (a) Polar plot, (b) Rectangular plot.

The directivity values for the 4 and 16-elements PAA are 5.6418, 11.7050 respectively. Although the level of the sidelobes are reduced, but the directivity is worse.

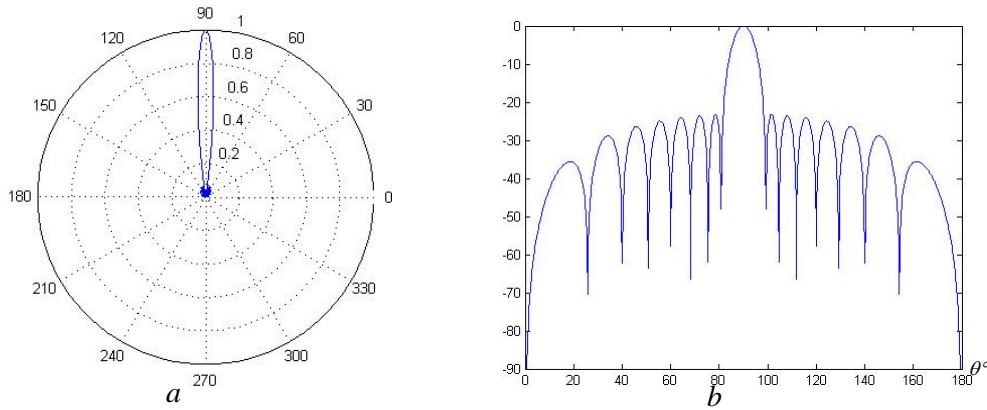


Fig. (11) The beam pattern of 16-elements PAA with Taylor Amplitude weighting  $MRA = 90^\circ$ , (a) Polar plot, (b) Rectangular plot.

### 3.3 Simulation of 4 and 16-Elements Array with Blackman-Harris Amplitude Weighting Function:

Blackman-Harris weighting simply extends the procedure to higher order harmonics to provide nulls at the peaks of the first two sidelobes. The weighting function is [Van Trees 2002]

$$w(n) = 0.42 + 0.5 \cos\left(\frac{2\pi n}{N}\right) + 0.08 \cos\left(\frac{4\pi n}{N}\right), \quad n = -\frac{N-1}{2}, \dots, \frac{N-1}{2} \quad (32)$$

The beam pattern characteristics of an  $N$ -element PAA with a Blackman-Harris spectral window can be calculated using the following mathematical equations [Rosario 2005]:

$$\Theta_{BW} = 1.65 \frac{2}{N}, \text{ Beam width} \quad (33)$$

$$SLL_{dB} = -56.6, \text{ SideLobe Level} \quad (34)$$

$$D_{dB} = 10 \cdot \log_{10}(N \cdot 0.577), \text{ Directivity} \quad (35)$$

The simulation for this spatial filter is shown in Figs. (12, 13) for the 4, and 16 PAA.

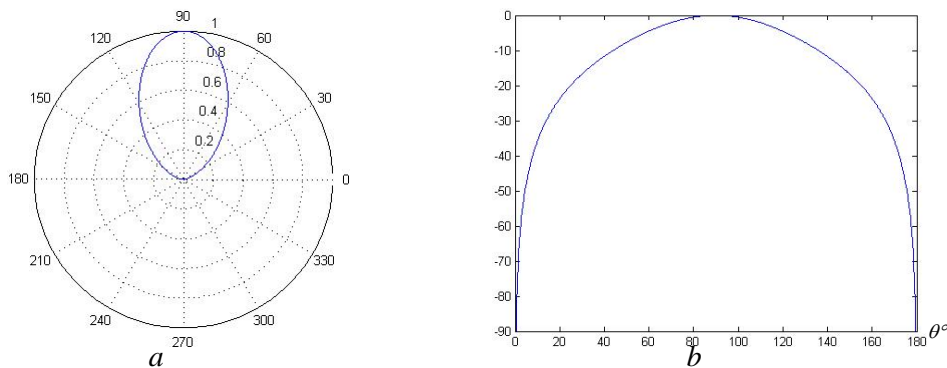


Fig. (12) The beam pattern of 4-elements PAA with Blackman-Harris Amplitude weighting  $MRA = 90^\circ$ , (a) Polar plot, (b) Rectangular plot.

The directivity  $D=3.6942, 9.6689$  for the 4 and 16-elements arrays respectively. The  $SLL$  is greatly reduced but  $D$  still less than the uniform weighting.

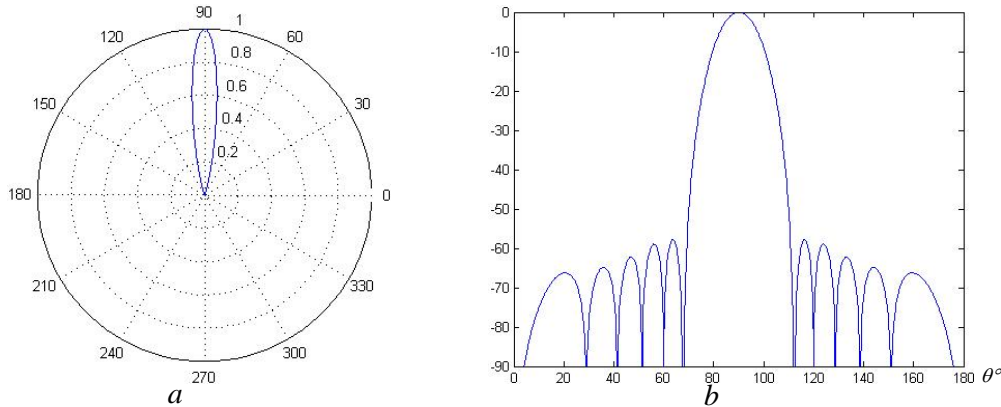


Fig. (13) The beam pattern of 16-elements PAA with Blackman-Harris Amplitude weighting  $MRA= 90^\circ$ , (a) Polar plot, (b) Rectangular plot.

**4. 2-D Array DBF Receiver:**

The PAA consists of 16 elements located along the x-y axes as shown in Fig. (14).

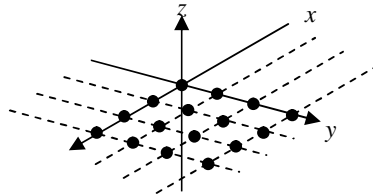


Figure (14) The 16 element array topology

The wavenumber  $k$  for each element of the array is [Van Trees 2002, Li and Stoica 2006, Rosario 2005]

$$\bar{k} = \frac{2\pi}{\lambda} \begin{bmatrix} \sin(\theta)\cos(\varphi) \\ \sin(\theta)\sin(\varphi) \\ 0 \end{bmatrix} \quad \bar{p} = \begin{bmatrix} p_x \\ p_y \\ 0 \end{bmatrix} \tag{36}$$

where  $\theta$  and  $\varphi$  are the azimuth and elevation for the incident wave front. We shall assume the wave front planar and a narrow band wave for the coming analysis.

**4.1 Uniform Weighting 2D 16-Elements PAA:**

Assuming a uniform weighting PAA for the 2-D PAA, the radiation pattern and the polar power distribution is shown in Fig.(15). In this simulation,  $\theta = 0^\circ, \varphi = 0^\circ$

The PAA assumed is  $4 \times 4$  array. From Fig. (14. b) we can see that the main beam power is concentrated in the origin of the contour plot.

To calculate the weights for this array, consider the general weight function given below [Van Trees 2002, Li and Stoica 2006, Rosario 2005]

$$w^* = \frac{1}{N} e^{jk^T(\theta_{MRA}, \varphi_{MRA}) \bar{p}_n} \tag{37}$$

Combining Eq.(36) and Eq.(37) yields:

$$w^* = \frac{1}{N} e^{j\left(\frac{2\pi}{\lambda}\right)\sin(\theta_{MRA})[p_x \cos(\varphi_{MRA}) + p_y \sin(\varphi_{MRA})]} \quad (38)$$

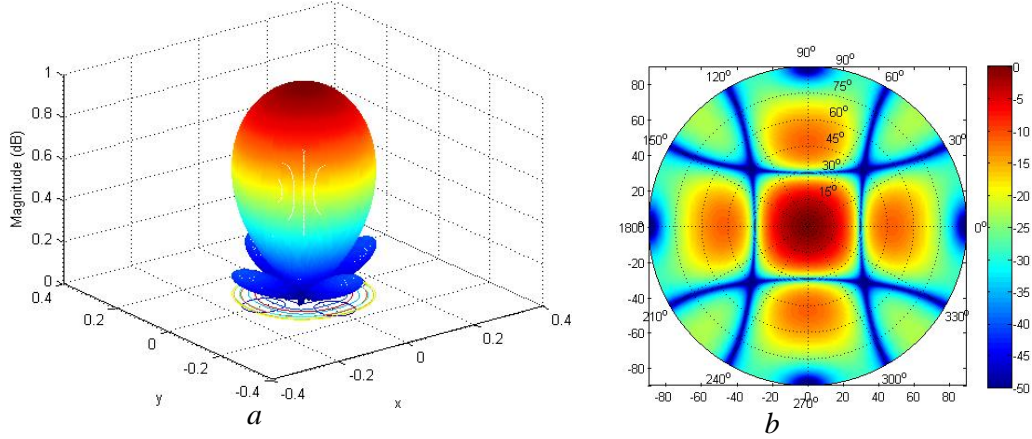


Fig. (15) (a) The 3d beam pattern, (b) Polar power distribution.

The phase value found in each weight coefficient can be viewed as the sum of the phase differences between neighboring elements in the same  $x$  axis value and phase difference between neighboring elements in the same  $y$  axis of the rectangular array. The relationship can be seen by restructuring Eq. (38) into the following mathematical form:

$$w^* = \frac{1}{N} e^{j(\Delta\psi_x + \Delta\psi_y)} \quad (39)$$

where

$$\Delta\psi_x = \left(\frac{2\pi}{\lambda}\right)p_x \sin(\theta_{MRA})\cos(\varphi_{MRA}) \quad (40)$$

$$\Delta\psi_y = \left(\frac{2\pi}{\lambda}\right)p_y \sin(\theta_{MRA})\sin(\varphi_{MRA}) \quad (41)$$

The weights for this array are given in Table 3.

Table 3 Complex weights of uniform weight 16-element 2D-PAA

Element	Weight	Element	Weight	Element	Weight	Element	Weight
1	0.0625	5	0.0625	9	0.0625	13	0.0625
2	0.0625	6	0.0625	10	0.0625	14	0.0625
3	0.0625	7	0.0625	11	0.0625	15	0.0625
4	0.0625	8	0.0625	12	0.0625	16	0.0625

The directivity  $D = 22.4253$  dB. The imaginary part = 0 because  $\sin(\theta) = \sin(\varphi) = 0$

#### 4.2 Dolph-Chebyshev Weighting 2D 16-Elements PAA:

The method that is discussed in this section was introduced by Dolph. Dolph-Chebyshev distribution method generates the amplitude of weight coefficients to minimize the MRA's beamwidth based on constant sidelobe level specifications. The Dolph-Chebyshev weighting function start with [Van Trees 2002, Li and Stoica 2006, Rosario 2005]

$$x_0 = \cosh\left(\frac{\cosh^{-1}(R)}{L-1}\right) \quad (42)$$

where  $R$  is defined as:

$$R = \frac{\text{mainlobe maximum}}{\text{SideLobe Level}} \tag{43}$$

$L$ : is the number of elements along one of the axes of the rectangular array.

The beam pattern for a rectangular PAA with  $L$ -elements along  $x$ -axis and  $M$ -elements along the  $y$ -axis is

$$B_{\psi}(\psi_x, \psi_y) = T_{L-1}\left(x_0 \cos\left(\frac{\psi_x}{2}\right) \cos(\psi_y)\right) \tag{44}$$

where  $T$  is the Chebychev polynomial.  $\psi_x, \psi_y$  are given in Eqs. (40, 41). The weights are calculated as follows:

$$w(l, m) = b(l, m) e^{-j\left[l\pi\left(\frac{L-1}{L}\right) + m\pi\left(\frac{M-1}{M}\right)\right]} \tag{45}$$

$b(l, m)$  can be found by applying Inverse Discrete Fourier Transform IDFT to  $B(k_1, k_2)$

$l, m$  represent the index of the location of the element.

The simulation was carried out for  $\theta = 0^\circ, \phi = 0^\circ$  and  $R=10$  dB. The results are shown in Fig. (16)

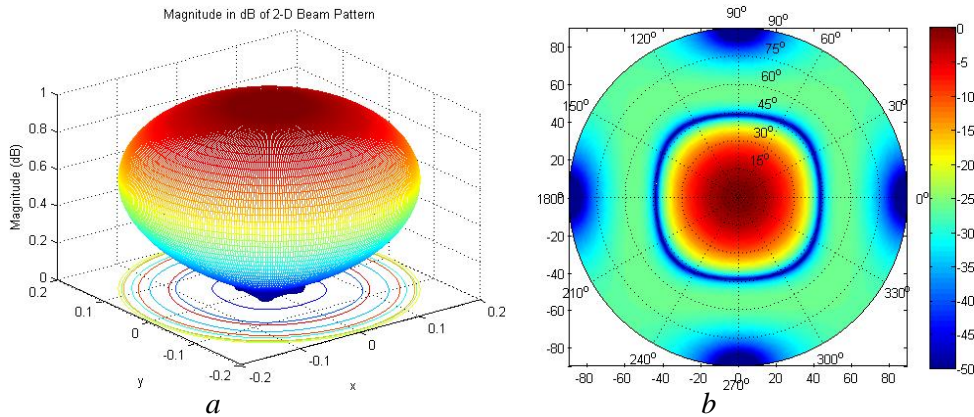


Fig. (16) (a) The 3d beam pattern, (b) Polar power distribution.

We can see from Fig. (15. b) that the main beam power is concentrated at the origin of the contours. Comparing it to Fig. (15. b), the main beam is widened but the SLL are highly suppressed. The directivity  $D=18.7929$  dB. The weights are shown in Table 3.

Table 4 Complex weights of Dolph-Chebychev weight 16-element 2D-PAA

Element	Weight	Element	Weight	Element	Weight	Element	Weight
1,1	0.0200	2,1	0.0599	3,1	0.0599	4,1	0.0200
1,2	0.0599	2,2	0.1101	3,2	0.1101	4,2	0.0599
1,3	0.0599	2,3	0.1101	3,3	0.1101	4,3	0.0599
1,4	0.0200	2,4	0.0599	3,4	0.0599	4,4	0.0200

### 5. Null Steering:

In many radar and communication systems there are signals that jam or create a high interference to the desired signal. For this reason we need to steer the nulls towards the angles of these unwanted signals to mitigate their effect and increasing SNR or SIR (Signal to Interference Ratio). For an arbitrary array, to put a null at  $M$  points, the wave number  $\mathbf{k}_i$  must satisfy the (zero- order) null constraint: [Allen and Ghavami 2005, Van Trees 2002, Jeffrey *et. al.*, Hemmati 2007, Ravishankar 2007]

$$\mathbf{w}^H \mathbf{v}(k_i) = 0, i = 1, \dots, M-1 \tag{46}$$

where

$\mathbf{w}$ : is the weight vector

$\mathbf{v}$ : is the array manifold vector

$^H$ : is the Hermitian operator

The  $N \times M$  constraint matrix  $\mathbf{C}$  is defined as

$$\mathbf{C} = [\mathbf{v}(k_1) \quad \mathbf{v}(k_2) \quad \dots \quad \mathbf{v}(k_M)] \quad (47)$$

Let  $\mathbf{w}_d$  be the set of desired weights with the corresponding pattern  $B_d(u)$ . Define an auxiliary weight vector  $\mathbf{A}$  as:

$$\mathbf{A} = \mathbf{w}^H \mathbf{C} (\mathbf{C} \cdot \mathbf{C}^H)^{-1} \quad (48)$$

The output pattern is

$$B_o = B_d - \sum_{i=1}^M a_i \frac{\sin\left(N\pi(u - u_i)/2\right)}{\pi(u - u_i)/2} \quad (49)$$

where  $u_i$  is the null direction corresponding to  $\mathbf{k}$ .

A simulation program was run with the following parameters,  $MRA=110^\circ$ ,  $L=4$ ,  $\nu=10^\circ$ ,  $40^\circ$  and  $60^\circ$ . The results are shown in Fig. (17)

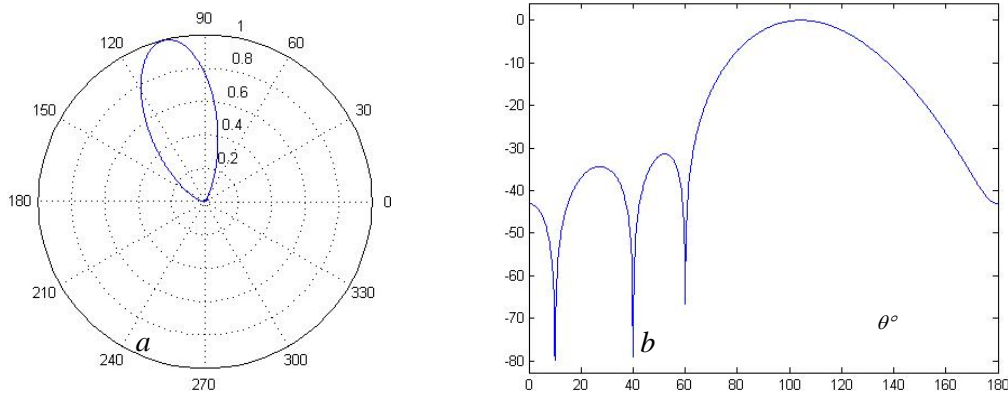


Fig. (17) Nulls at 10, 40 and 60, (a) Polar plot, (b) Cartesian plot

For 2-D  $4 \times 4$  array PAA antenna, with  $MRA=20^\circ$ ,  $MRA=40^\circ$  and nulls at  $\theta_{null}=80^\circ$ ,  $\theta_{null}= -30^\circ$  and Dolph-Chebyshev weight spatial filter, the simulation results are shown in Fig. (18). Null Cartesian location is at  $u_x=0.8529$ ,  $u_y= -4.924$

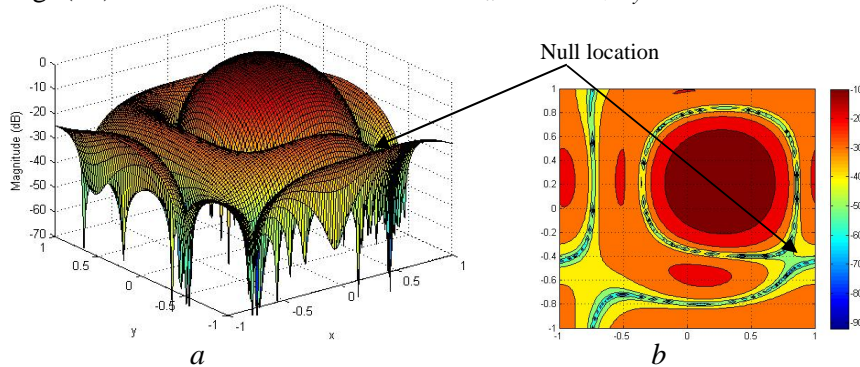


Fig. (18) Null placement for  $4 \times 4$  array PAA antenna with Dolph-Chebyshev weight spatial filter (a) 3-D plot, (b) Contour plot

## 6. Conclusions:

Digital Beamforming receiver represents a major step in the design of receiving antenna. When high baudrates ADC are devised, the whole receiving PAA could be constructed using softwares only. The conversion of received data to digital format makes it very possible to apply the DSP operation on the data received. The DSP can be implemented using FPGA or dedicated processor. The sifted sideband beamforming requires less data storage capacity but extra complexity is added. The CIC is used when it is needed to provide the necessary compatibility between devices with different baudrates. The spatial filter has a high influence on the final radiation pattern. The uniform spatial filter has the highest directivity but with high SLL. The sidelobes can be greatly reduced using different spatial filters but on the cost of directivity. The spatial filter either assumes a constant SLL or variable SLL with minimum beamwidth. If an interference or jamming combating the array from a certain angle, the effect can be reduced by steering the nulls towards that angle.

### References:

B. Allen and M. Ghavami, *Adaptive Array Systems Fundamentals and Applications*, John Wiley & Sons, Ltd, 2005.

Chen Sun, Jun Cheng, and Takashi Ohira, *Handbook on Advancements in Smart Antenna Technologies for Wireless Networks*, Information science reference N.Y. 2009.

David C. Swanson, *Signal Processing for Intelligent Sensor Systems*, Marcel Dekker, Inc., 2000.

Gerhard Krieger, Nicolas Gebert, and Alberto Moreira “Multidimensional Waveform Encoding: Anew Digital Technique for Synthetic Aperature Radar Remote Sensing”, *IEEE Transaction on Geoscience and Remote Sensing*, Vol. 46, No.1, Jan. 2008.

Harry L. Van Trees, *Optimum Array Processing Part IV of Detection, Estimation, and Modulation Theory*, John Wiley & Sons, Inc., 2002.

Jeffrey Foutz, Andreas Spanias, and Mahesh K. Banavar, *Narrowband Direction of Arrival Estimation for Antenna Arrays*, Morgan and Claypool 2008.

Jian Li and Petre Stoica, *Robust Adaptive Beamforming*, John Wiley & Sons, INC., 2006.

John Litva and Titus Kwok-Yeung Lo, *Beamforming in Wireless Communications*, Artech House, INC., 1996.

Juan A. Torres-Rosario, “Implementation of a Phased Array Antenna Using Digital Beamforming”, *M.Sc. Electrical Engineering, Uniresity of Puerto Rico*, 2005.

Karin Schuler, Marwan Younis, Rainer Lenz, Werner Wiesbeck, “Array Design for Automotive Digital Beamforming Radar System”, *IEEE International Radar Conference*, 2005.

---

Lal C. Godara, “ Application of Antenna Arrays to Mobile Communications, Part II: Beam-forming an Direction-of-Arrival Considerations”, *Proceedings of the IEEE*, Vol. 85, No. 8, 1997.

Ronald A. Godara, “A comparison of Efficient Beamforming Algorithms”, *IEEE Transaction on Acoustics, Speech, and Signal Processing*, Vol. ASSP-32, No. 3, 1984.

S. Ravishankar, H. V. Kumaraswamy, and B. D. Satish, “The Selection of Weighting Functions For Linear Arrays Using Deferent Techniques, *National Conference on Electronic s and Communication Pune*, 2007.

Varahram Hemmati, “Null and Beam Steering Performance of Rectangular Arrays with Dolph-Chebyshev Weighting”, *Contract Report DRDC Ottawa CR 2007-194*, Defence R&D Canada – Ottawa, October 2007.

Wins Ton Li and Xin Pin Ghuang, “Performance Evaluation of Digital Beamforming Strategies for Satellite Communications”, *IEEE Transactions on Aerospace and Electronic Systems*, Vol. 40, Issue 1, Jan 2004.

Wulf-Dieter Wirth, *Radar techniques using array antennas*, The Institution of Electrical Engineers, London 2001.

Zheng Shenghua, Xu Dazhuan ,Jin Xueming, “A New Receiver Architecture for Smart Antenna with Digital Beamforming” *IEEE International Symposium on Microwave, Antenna, Propagation and EMC Technologies for Wireless Communications Proceedings*, 2005.